

# **A NEW METHOD OF FITTING APPROXIMATE VIBRATIONAL SPECTRA TO HEAT CAPACITIES OF SOLIDS WITH TARASOV FUNCTIONS**

*Ge Zhang and B. Wunderlich*

Division of Analytical and Chemical Sciences, Oak Ridge National Laboratory, Oak Ridge, TN 37831-6197; and Department of Chemistry, University of Tennessee, Knoxville, TN 37996-1600, USA

## **Abstract**

A new, least-squares optimization method with interpolation is devised to fit skeletal vibrational heat capacities to the two parameters  $\Theta_1$  and  $\Theta_3$  in the Tarasov function used for heat capacity calculations of linear macromolecules. When heat capacities are available in the proper temperature range,  $\Theta_1$  and  $\Theta_3$  can be determined uniquely in a single computer run. Appended to our Advanced THERMAL Analysis System (ATHAS), this new method offers an improvement in analyzing heat capacity data and facilitates the systematic study of the physical significance of  $\Theta_1$  and  $\Theta_3$  values for all polymers and related molecules of the ATHAS data bank.

**Keywords:** heat capacity, least-squares fitting, Tarasov function, vibration frequency spectrum

## **Introduction**

Heat capacities of macromolecules in the solid state have been characterized in a variety of ways. One of the most widely used approximate method is the Tarasov analysis. In this approach, a combination of one- and three-dimensional Debye functions is chosen to model the skeletal heat capacities of linear molecules and to compute their temperature dependence [1]. Incorporating the Tarasov approach, the Advanced THERMAL Analysis System (ATHAS) has been developed in our laboratory for the evaluation of the thermal properties of linear macromolecules and related compounds, and to maintain a critically evaluated data bank [2]. As a result of these efforts, detailed thermodynamic information exists now for over 200 linear macromolecules and related small molecules. The ATHAS permits to link the macroscopic heat capacities to their microscopic cause. At low temperature, this cause is practically exclusively vibrational motion. As the temperature increases, large-amplitude motion may become possible, usually in the form of conformational motion (internal rotation) and, for small molecules, also rotation and translation. Often, this large-amplitude motion begins at a well-defined phase transition (melting, glass transition, or disordering transition). Recently, it could be shown, however, that

more complicated molecules, particularly those which display mesophases, may also gradually gain large-amplitude mobility at temperatures far below the disordering transitions [3]. To identify such gradual gain of large-amplitude motion, one compares the measured heat capacity with the heat capacity expected for vibrations-only and makes a general accounting of the changes in entropy found and expected for various types of mobility and disorder.

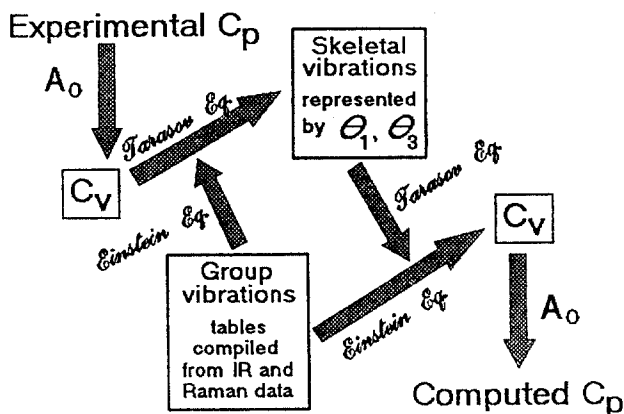


Fig. 1 Schematic of the ATHAS for solids, leading on the basis of experimental heat capacities over a limited temperature range to computed full range data. The method is based on fitting to an approximate vibration spectrum

To achieve a full characterization, the measured low-temperature heat capacities are first fitted to approximate vibration spectra in the sequence shown in the left half of Fig. 1 and described in detail below. Then, the vibrational heat capacities are calculated for the higher temperature range, using the low-temperature-fitted skeletal and group vibration spectrum. Figures 2 and 3 show, for example, the deviations of the measured heat capacities of glassy and crystalline polyethylene from the heat capacities expected from vibrations only (shaded areas) [4, 5]. Both experimental data sets were obtained by extrapolation of partial crystallinity to the amorphous and crystalline states, respectively [6]. The increase in experimental heat capacity could be linked to the beginning of local *gauche-trans* mobility in this temperature region. In glassy polyethylene it begins already at about 120 K, while in crystalline polyethylene it begins at about 275 K. The deviations of the heat capacity from the vibrational  $C_p$  were already observed in 1963 and were the reason for the development of ATHAS [7]. For the crystalline polyethylene the *trans-gauche* conversions could be documented also by IR analyses, and by molecular dynamics simulation [8, 9].

The Debye functions contained in the Tarasov function are, however, not available in closed forms, an inversion of heat capacities to the approximate vibration spectrum can, thus, only be done by trial and error [10]. The technique to extract the parameters for the Tarasov equation from experimental data is

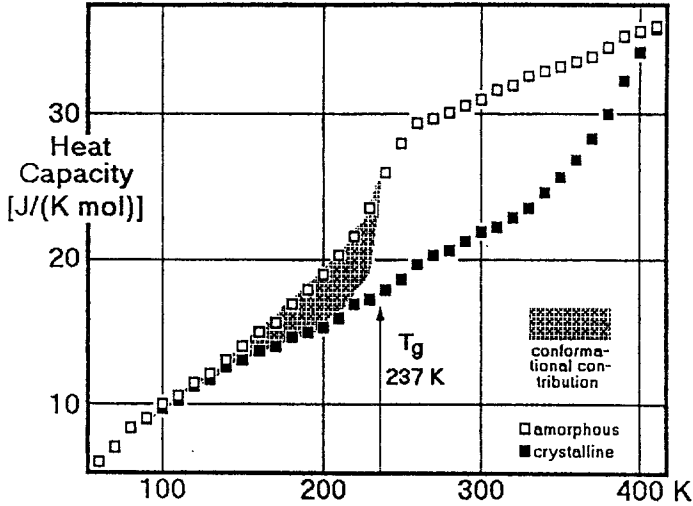


Fig. 2 Experimental  $C_p$  of amorphous polyethylene, compared to the vibration-only, computed  $C_p$ . Shaded area indicates the  $C_p$ -contribution of large-amplitude motion

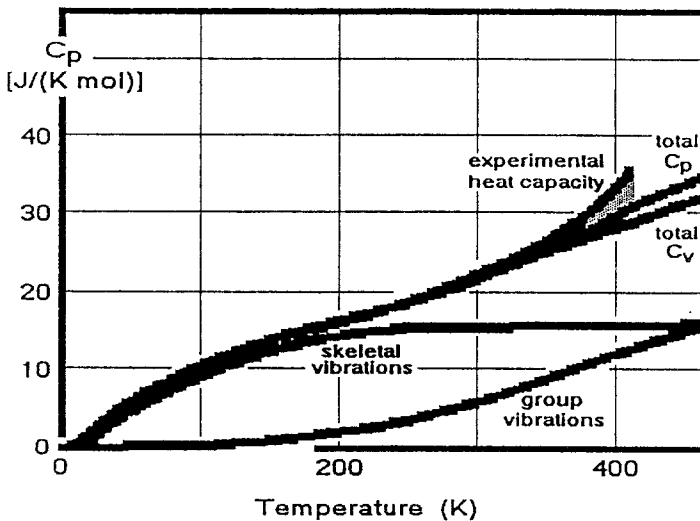


Fig. 3 Experimental  $C_p$  of crystalline polyethylene, compared to the vibration-only, computed  $C_p$ . Shaded area indicates the  $C_p$ -contribution of large-amplitude motion

often tedious and suffers from accuracy problems. A neural network program was recently prepared to simplify the task [11]. Although it gives improved results and seems independent of personal judgement, it is not sufficiently transparent to safely interpret the obtained  $\Theta$ -temperatures. In the present paper a new method is described that involves a direct least-squares fitting method with interpolation that can optimize the two parameters of the Tarasov function,

$\Theta_1$  and  $\Theta_3$ . For testing purposes, several representative polymers, for which low temperature data of heat capacity at constant pressure,  $C_p$ , exist, were selected. In addition, three sets of computed  $C_p$  data from assumed frequency spectra were analyzed. For every set of data, one, and only one, pair  $\Theta_1$  and  $\Theta_3$  for the Tarasov function representing the skeletal vibrational contribution to the heat capacity are obtained by this new optimization method together with the error in  $C_p$  of the best fit. The method can be applied to all polymers of the ATHAS data bank and should lead to an improved set of correlations.

## Heat capacity theory

The historical perspective of heat capacities for idealized models is well known and will not be discussed here [12]. For macromolecules, it has been found that group vibrations contribute little to low temperature heat capacities at constant volume,  $C_v$ , and are well approximated using a summation of Einstein functions [13], which are given in units of  $NR$  by:

$$C_v/NR = E(\Theta_E/T) = \frac{(\Theta_E/T)^2 \exp(\Theta_E/T)}{[\exp(\Theta_E/T) - 1]^2} \quad (1)$$

where  $R$  is the gas constant and  $N$ , the number of vibrators. For the skeletal vibrations, it has been found that their heat capacity contribution can be approximated by a combination of Debye functions. The one, two and three-dimensional Debye functions  $D_1$ ,  $D_2$  and  $D_3$  are given by:

$$C_v/NR = D_1(\Theta_1/T) = (T/\Theta_1) \int_0^{(\Theta_1/T)} \frac{(\Theta/T)^2 \exp(\Theta/T)}{[\exp(\Theta/T) - 1]^2} d(\Theta/T) \quad (2)$$

$$C_v/NR = D_2(\Theta_2/T) = 2(T/\Theta_2)^2 \int_0^{(\Theta_2/T)} \frac{(\Theta/T)^3 \exp(\Theta/T)}{[\exp(\Theta/T) - 1]^2} d(\Theta/T) \quad (3)$$

$$C_v/NR = D_3(\Theta_3/T) = 3(T/\Theta_3)^3 \int_0^{(\Theta_3/T)} \frac{(\Theta/T)^4 \exp(\Theta/T)}{[\exp(\Theta/T) - 1]^2} d(\Theta/T) \quad (4)$$

respectively. The Debye function  $D_1(\Theta_1/T)$  is based on a constant frequency distribution,  $D_2(\Theta_2/T)$  on a linear distribution, and  $D_3(\Theta_3/T)$  on a quadratic distribution. The parameters  $\Theta_1$ ,  $\Theta_2$  and  $\Theta_3$  are the characteristic upper frequencies for these approximations to the density of vibrational states and represent  $h\nu/k$ , where  $h$  is Plank's constant and  $k$  is Boltzmann's constant ( $1 \text{ K} = 0.695 \text{ cm}^{-1}$ ).

Using a combination of Eqs (2) and (4) to approximate the skeletal heat capacities of macromolecules, Tarasov has proposed the form [1]:

$$C_v/NR = T(\Theta_1/T, \Theta_3/T) = D_1(\Theta_1/T) - (\Theta_3/\Theta_1)[D_1(\Theta_3/T) - D_3(\Theta_3/T)] \quad (5)$$

to model the function  $C_v(T)$ . We have successfully used this approach in the ATHAS for a variety of polymer systems. It turns out, however, that the inversion of  $C_v$  vs.  $T$  to  $\Theta_1$  and  $\Theta_3$  is not trivial and requires a complex procedure. In this paper, a straight-forward, least-squares fitting method with interpolation is presented.

## Calculations

The ATHAS computation scheme is briefly explained as follows: The vibrational spectra of solid polymers are separated into group and skeletal vibrations ( $N = \text{number of atoms} \times 3 = N_g + N_s$ ). The number and types of group vibrations,  $N_g$ , are derived by inspection of the chemical structure, and are then represented by a series of single frequencies and/or box-distributions over narrow frequency ranges. These frequencies can be taken from normal-mode calculations on isolated chains that are fitted to experimental IR and Raman frequencies of the macromolecule or suitable low molecular mass analogs. The remaining number of skeletal vibrations,  $N_s$ , are not well represented by present-day normal-mode calculations, but can be approximated for linear molecules by fitting the experimental, low-temperature skeletal heat capacities to the Tarasov function with two parameters,  $\Theta_1$  and  $\Theta_3$ . Most sensitive in the 100–300 K temperature region, the parameter  $\Theta_1$  governs the contributions of a constant frequency distribution (box), largely representative of the intramolecular vibrations; while most sensitive in the 0–50 K governs region,  $\Theta_3$  does the same for a quadratic frequency distribution, largely representative of the intermolecular chain vibrations [10, 14]. Prior to each fitting, the measured  $C_p$  is converted to  $C_v$  and the computed group vibrational contribution is subtracted, leaving the experimental skeletal component to be represented by the Tarasov function (Fig. 1, left). The resulting approximate vibrational spectrum, consisting of group and skeletal vibrations (the latter defined by the optimized  $\Theta_1$  and  $\Theta_3$ ), is then inverted back to give the computed heat capacities at constant volume  $C_v$  (Fig. 1, right). To convert the experimental  $C_p$  to  $C_v$ , and *vice versa*, one can use the well-known thermodynamic relationship. Since expansivity and compressibility are, however, not known for most of the polymers, one needs to use the modified Nernst-Lindemann approximation that was proven applicable for polymers [15]:

$$C_p - C_v = 3RA_0(C_p T/T_m^0) \quad (6)$$

where  $A_0$  is an approximate universal constant [ $3.9 \times 10^{-3}$  (K mol) $J^{-1}$ ], and  $T_m^0$  refers to the equilibrium melting temperature. The difference between  $C_p$  and  $C_v$  decreases rapidly with temperature, so that below 60 K its contribution to the heat capacity is less than 1.0% for most polymers and  $C_p$  could be used directly for the evaluation of  $\Theta_1$  and  $\Theta_3$  [10].

The new least-squares optimization method for obtaining  $\Theta_1$  and  $\Theta_3$  of the Tarasov function is, in fact, conceptually very simple. Briefly, an appropriate merit function that describes the goodness of fit is optimized (usually minimized) by adjusting the parameters until all preset fitting criteria are satisfied. In this work, the root mean square (*rms*) error,  $\Delta$ , between the experimental ( $C_{\text{exp}}$ ) and calculated ( $C_{\text{calc}}$ ) heat capacities is chosen to be the merit function. Then  $\Delta$  is optimized for the least value by varying the two Tarasov parameters,  $\Theta_1$  and  $\Theta_3$ . The best fit and corresponding  $\Theta_1$  and  $\Theta_3$  are thus determined through this least-squares fitting procedure and  $\Delta$  is computed for  $N$  data points. The relative *rms* error is given by:

$$\Delta = \sqrt{\frac{\sum_{i=1}^N \left( \frac{C_{\text{calc}}(T_i) - C_{\text{exp}}(T_i)}{C_{\text{exp}}(T_i)} \times 100 \right)^2}{N}} \quad (7)$$

Since the Tarasov function is not only nonlinear, but contains also several integrations of nonclosed form, common least squares optimization algorithms do not apply well in fitting for  $\Theta_1$  and  $\Theta_3$ . An alternative is to go back to the primitive approach of locating the minimum of the least squares by making a complete survey of the parameter domain space. First the possible range of values for  $\Theta_1$  and  $\Theta_3$  are divided into  $m$  and  $n$  equal parts, respectively. The two-dimensional parameter space is thereby separated into  $m \times n$  cells. Equal numbers of steps are used in our case to simplify the computation ( $m = n$ ). A complete survey means we have to first calculate the value of  $\Delta$  at every grid point ( $\Theta_1$ ,  $\Theta_3$ ). By comparing all the values obtained, the least or first order minimum of  $\Delta$  can be located. The actual computer program is constructed based on a standard algorithm, often used for energy minimization in physics [16].

With information provided by our ATHAS data bank, a 20 by 20 mesh is selected in the two-dimensional parameter domain space, with  $\Theta_1$  from 200 to 960 K in step of 40 K, and  $\Theta_3$  from 10 to 200 K in steps of 10 K. The 400 grid points made of the sets of ( $\Theta_1$ ,  $\Theta_3$ ) are then evaluated for their fit to the heat capacity. The output for each ( $\Theta_1$ ,  $\Theta_3$ ) is the *rms* error  $\Delta$  of Eq. (7) from the comparison with the heat capacities over the complete temperature range of available data or data of interest. Both absolute or relative errors can be used as fitting criteria. The latter case is shown in Eq. (7) and is used for this study. The mesh is therefore evaluated for the *rms* error  $\Delta$  of fitting the experimental  $C_p$  to the Tarasov function.

The least among all  $\Delta$  values and its corresponding  $(\Theta_1, \Theta_3)$  are the best fit if the test data sets are sufficient for the fitting criteria. Usually this condition cannot be met due to consideration of efficiency, computer time and storage space limitation. The accuracy of such an approach is then limited by the number of subdivisions we can take for each parameter. Furthermore, the amount of computation and storage requirement can be large, even for modest values  $m$  and  $n$ . It is, thus, not practical to evaluate all possible combinations of  $\Theta_1$  and  $\Theta_3$ , even if a recursive searching scheme with ever finer grid spacing is utilized. As remedies, it is possible to modify the method into an interactive search, instead of the fixed grid, or to combine it with a fine-search, using a direct interpolation around the first-order minimum of  $\Delta$  reached at a grid point. The approach using the direct interpolation is best suited to our problem. To proceed, the mesh point with the least fitting error is identified together with its neighboring points. A standard interpolation method is then employed to estimate the global minimum between the mesh points. Integration of all relevant functions is performed by the subroutine D01AHF based on the Patterson method [17] listed in the Fortran Math Library of the Numerical Algorithm Group (NAG) [18]. Typical running times for fitting the data for one polymer are less than one-half minute on a typical mainframe VAX 6000-440 computer.

## Results

The representative polymers and small molecules chosen for analysis were polyethylene (PE), poly(propylene) (PP), polytetrafluoroethylene (PTFE), poly(vinyl chloride) (PVC), polystyrene (PS), poly(oxymethylene) (POM), poly(methyl methacrylate) (PMMA), poly(ethylene terephthalate) (PET), propane, polymethionine (PMET), polyphenylalanine (PPHE), bovine zinc insulin dimer, and bovine chymotripsinogen A. The data selected referred either the crystalline or amorphous solid states, or, when available, both crystal and glass were analyzed. The poly(amino acid) and the protein heat capacities refer to anhydrous samples. Three sets of simulated data for polyethylene with computed skeletal heat capacity contributions were also included in the analysis. These simulated data were the same as used before in the testing of the neural network method for the prediction of  $\Theta_1$  and  $\Theta_3$  [11]. All chosen examples have low temperature  $C_p$  data available in the ATHAS data bank [2].

The results of the fittings are listed in Table 1. The key parameters are  $\Theta_1$ ,  $\Theta_3$  and  $\Theta_D$ , where  $\Theta_D$  is the Debye temperature, obtained by fitting Eq. (4) at low temperatures ( $< 50$  K). The number of skeletal vibrations  $N_s$ , the average (av) and root mean square (rms) errors, and the temperature range of fitting are also listed in Table 1. For the data sets that were analyzed before by the old estimation method and for the simulated data, the prior known  $\Theta_1$ ,  $\Theta_3$ , and  $\Theta_D$  are listed in parentheses. Figures 4–7 show some typical plots of the fittings.

**Table 1**  $\Theta_1$  and  $\Theta_3$  values of optimization

Polymer	$N_s$	$\Theta_1/K^a$	$\Theta_3/K^a$	$\Theta_D/K^a$	% av & rms error <sup>b</sup>	Temp./K <sup>c</sup>
PE cryst	2	529(519)	160(158)	238(235)	1.1±2.1	1.8–300.0
PE amorph	2	586(519)	71(80)	143(149)	-1.4±5.9	5.0–110.0
PP cryst	7	719(714)	103(91)	197(181)	0.4±3.0	10.0–300.0
PP amorph	7	643(633)	75(78)	153(157)	0.2±3.7	10.0–260.0
PTFE cryst	2	276(250)	50(54)	89(90)	-1.4±3.8	1.0–250.0
PVC amorph	4	358(354)	50(45)	97(89)	-0.6±3.8	5.0–350.0
PS amorph	6	282(284)	50(48)	90(87)	-0.4±4.8	0.7–300.0
POM cryst	2	225(232)	119(117)	147(147)	-3.4±5.3	2.0–300.0
PMMA amorph	14	681(680)	87(67)	173(145)	0.8±1.9	10.0–300.0
PET amorph	15	637(586)	43(44)	105(104)	-2.5±6.7	1.2–320.0
Propane	9	365(360)	131(128)	185(181)	-0.6±4.8	15.0–80.0
PMET	15	542	83	155	-0.5±1.6	5.0–200.0
PPHE	11	396	67	121	1.4±3.5	5.0–300.0
Insulin	628	599	79	155	0.01±3.1	10.0–300.0
Chymotryps.	3005	631	79	158	0.5±3.2	10.0–300.0
Simulation 1	2	447(450)	152(150)	217(216)	0.2±2.2	3.0–300.0
Simulation 2	2	523(530)	192(190)	268(267)	0.3±2.2	3.0–300.0
Simulation 3	2	485(490)	111(110)	182(181)	0.1±0.7	3.0–300.0

<sup>a</sup> The data in parentheses give the old data bank values or the simulation input.

<sup>b</sup> Note that these errors refer to the total heat capacity  $C_p$  of the skeletal and group vibrations. Any error of group vibration assignment and  $C_p$ -to- $C_v$  conversion can naturally not be fully compensated by fitting  $\Theta_1$  and  $\Theta_3$ .

<sup>c</sup> Temperature range of the experimental or simulated data used for fitting.

## Discussion

The first observation is that the new data in Table 1 approach the corresponding old  $\Theta$  values (in parentheses) available for comparison. The simulation data indicate that the method is usually within the typical experimental error of 3–5%. In the previous standard ATHAS method, one took an average of the  $\Theta$ -temperatures obtained by point-by-point inversions in the temperature region where they appeared reasonably constant. The condition was to achieve a constant  $\Theta$ -temperatures over a chosen temperature range [10, 14]. Naturally, this choice of best  $\Theta$ -temperature does not necessary lead to the least error in heat capacity. In addition to unavoidable subjective choices affecting the results, the entire process is often lengthy and time consuming. The new optimization method, as shown in Figs 4–7, is considerably more efficient since



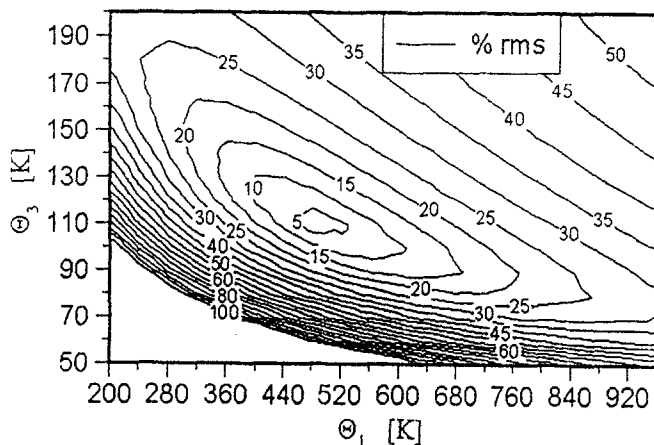


Fig. 4 Contour map of the fitting of the experimental heat capacity to a Tarasov function with parameters  $\Theta_1$  and  $\Theta_3$  for simulation #3 (PE-molecule,  $\Theta_1=490$  K)

both  $\Theta_1$  and  $\Theta_3$  are obtained in a single run and the fitting is directly linked to the error in  $C_v$ , where the percentage least-squares error of all data in the chosen temperature interval is calculated.

The plots in Figs 4–7 prove also the physical relevance of the two-parameter description. There is one and only one pair of optimal  $\Theta$ -values. Furthermore, the new method is inherently transparent, robust, objective, and easy to learn and use. Considering the accuracy, the final interpolation of the new method gives an estimated precision of one quarter of the spacing between neighboring grid points in the mesh. Hence it should not exceed 10 K for  $\Theta_1$  and 3 K for  $\Theta_3$ . The

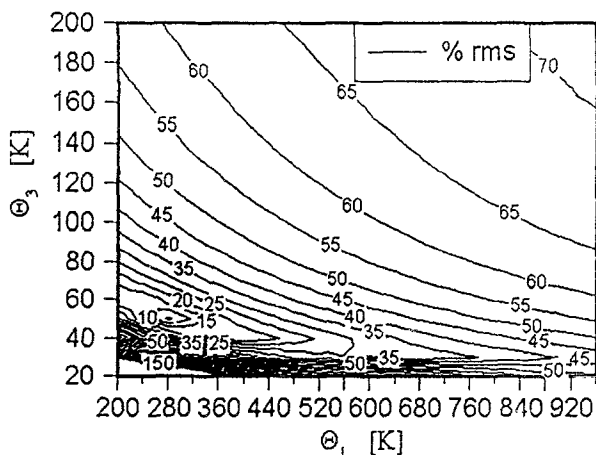


Fig. 5 Contour map of the fitting of the experimental heat capacity to a Tarasov function with parameters  $\Theta_1$  and  $\Theta_3$  for PTFE, crystalline

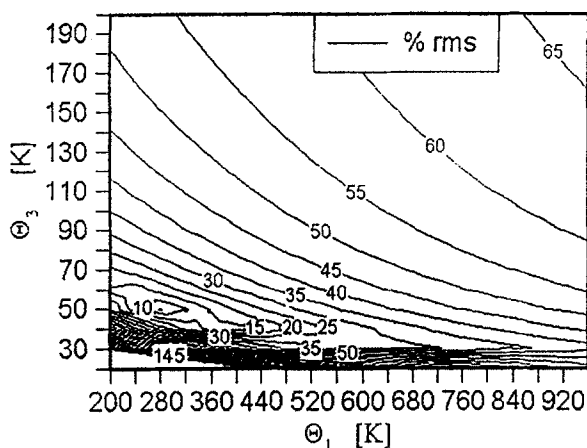


Fig. 6 Contour map of the fitting of the experimental heat capacity to a Tarasov function with parameters  $\Theta_1$  and  $\Theta_3$  for PS, amorphous

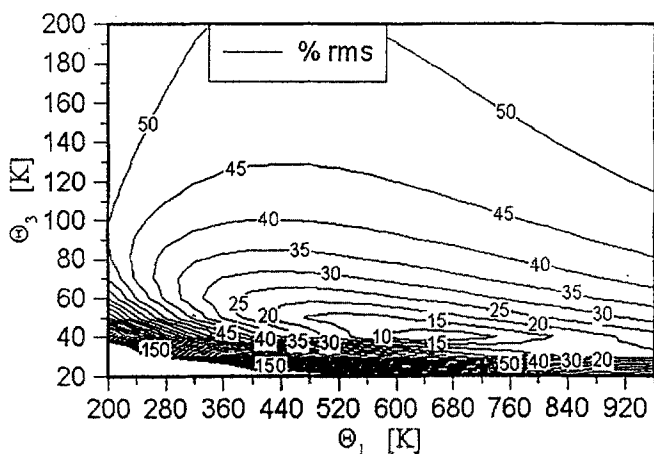


Fig. 7 Contour map of the fitting of the experimental, skeletal heat capacity to a Tarasov function with parameters  $\Theta_1$  and  $\Theta_3$  for PET, amorphous

experimental error usually associated with heat capacity measurement precludes the need for more precise theoretical parameters.

As a check of the results presented in this paper, one can look also at the connection between the old and new fitting scheme through the parameter  $\Theta_D$  which is  $\Theta_3$  of the 3-dimensional Debye function  $D_3$  [Eq. (4)]. At very low temperature, both  $D_3$  [Eq. (4)] and the Tarasov function Eq. (5) approach the well-known  $T^3$ -dependence of the heat capacity and, therefore, yield the same values for  $C_v$ . In other words, in the low temperature limit the following equation holds for Eqs (4) and (5) [10]:

$$C_v/NR = \left(\frac{4\pi^4}{5}\right) \left(\frac{T}{\Theta_D}\right)^3 = \left(\frac{4\pi^4}{5}\right) \left(\frac{T}{\Theta_3}\right)^2 \left(\frac{T}{\Theta_1}\right) \quad (8)$$

which can be simplified to:

$$\Theta_D^3 = \Theta_3^2 \Theta_1 \quad (9)$$

The  $\Theta_D$  values presented in Table 1 were computed using Eq. (9). They correspond accurately to the values found before by direct fitting at very low temperature.

The comparison between the new least-squares and the neural-network method is made by simply recalculating the simulated data used by Noid *et al.* [11]. The three sets of simulated  $C_p$  and one of experimental  $C_p$  for crystalline PE [6] that were used in the neural network inversion to  $\Theta_1$  and  $\Theta_3$  were also used in the current procedure and the new results are listed in Table 1. In all cases, similarly precise  $\Theta_1$  and  $\Theta_3$  were obtained as by the neural network methods (518.8, 156.9 for PE; 450.4, 148.6 for Sim. 1; 529.7, 191.0 for Sim. 2; and 489.4, 108.5 for Sim. 3). However, the real improvement lies in the fact that no rigid restriction on the type of polymers and the regularity, distribution and number of  $C_p$  data is necessary for the new method. The main advantage of the least-squares method is the simple conception and transparent calculation process towards any data set, whereas the neural network works more or less like a black box. Although promising as other neural network applications, the inversion of the Tarasov equation shares a few recognized, common problems as well. The undesirable lack of generalization and over-memorization often limits the method to polymers related to the training sets [19]. Whereas the new method, irrespective of the number of input data point, applies to any polymer or other solid state material. Despite the differences, there is one similarity between the two approaches, i.e., both utilize minimization algorithms to reach either the optimal parameters directly as in case of the new method, or the weight configuration for the neural network.

With the current method both the absolute and relative *rms* error can be used as criteria for the evaluation of the fitting quality. Adhering to different physical quantities, either choice usually yields very good  $\Theta_1$  and  $\Theta_3$  values according to preliminary tests. But, it remains to establish the changes in  $\Theta$ -values if absolute errors are used instead of percentage errors. The absolute errors would be of advantage for the optimization of the integral properties ( $H$ ,  $S$  and  $G$ ), while the percentage error is useful for the assessment of the heat capacity as a function of temperature.

The largest sensitivity in the  $\Theta$ -to- $C_v$  inversion is at the point of inflection of the Tarasov function, at about  $\Theta/4$  to  $\Theta/5$  [20]. For a  $\Theta_1$  of 400 to 550 K one expects highest accuracy at about 100 K, still somewhat below the usual experi-

mental temperature range. At higher temperatures the sensitivity of the inversion decreases and approaches zero above the  $\Theta$ -temperature as  $C_v$  approaches  $N_s \times R$  (Dulong-Petit's rule). It is therefore essential for an accurate  $C_p$  to  $\Theta$ -temperature inversion to include as many low temperature data as possible. The data tables and corresponding curves, as well as tables of the computed  $C_p$  and the recommended experimental  $C_p$  for the selected polymers can be inspected and reproduced from the ATHAS data bank, increasingly available through the World Wide Web on the Internet [2].

## Conclusions

We have presented a new method for extracting the  $\Theta_1$  and  $\Theta_3$  parameters in the Tarasov equation for modeling the temperature-dependence of  $C_v$  for the solid state macromolecules. This technique was demonstrated to lead to an accuracy of about 10 K for  $\Theta_1$  and 3 K for  $\Theta_3$ , which is an improvement over prior methods. More importantly, we have successfully complemented the ATHAS analysis framework with a fitting procedure of more systematic precision that facilitates the systematic study of the physical significance of  $\Theta_1$  and  $\Theta_3$  values over the entire ATHAS data bank. Using the theory-backed heat capacities, it is possible to arrive at a better knowledge of broad range transitions which are common in macromolecules. The variation of the  $\Theta$  temperatures from polymer to polymer is correlated so that, in case of missing data, first approximations can be estimated from the extensive tabulation in the ATHAS data bank.

\* \* \*

We are grateful to Dr. Jing-ye Zhang for discussions and help during the development of the minimization methods. Financially this work was supported by the Division of Materials Research, National Science Foundation, Polymers Program, Grant # DMR 90-00520 and the Division of Materials Sciences, Office of Basic Energy Sciences, U.S. Department of Energy, under Contract DE-AC05-84OR21400 with Lockheed Martin Energy Systems, Inc.

'The submitted manuscript has been authored by a contractor of the U.S. Government under the contract No. DE-AC05-84OR21400. Accordingly, the U.S. Government retains a nonexclusive, royalty-free license to publish or reproduce the published form of this contribution, or allow others to do so, for U.S. Government purposes.'

## References

- 1 V. V. Tarasov, Zh. Fis. Khim., 24 (1950) 111; 27 (1953) 1430; 39 (1965) 2077; and Dokl. Acad. Nauk SSSR, 100 (1955) 307.
- 2 ATHAS data bank. For a recent description see: B. Wunderlich, Pure and Appl. Chem., 67 (1995) 1019. For the data bank of experimental heat capacities see: U. Gaur, S.-F. Lau, H.-C. Shu, B. B. Wunderlich, M. Varma-Nair and B. Wunderlich, J. Phys. Chem. Ref. Data, 10 (1981) 89, 119, 1001, 1051; 11 (1982) 313, 1065; 12 (1983) 29, 65, 91; and (1990), 20 (1991) 349-404. For detailed information see World Wide Web address on the Internet: <http://funnelweb.utcc.utk.edu/~athas>.
- 3 A. Xenopoulos, J. Cheng and B. Wunderlich, Mol. Cryst. Liq. Cryst., 226 (1993) 87; Y. Jin, J. Cheng, B. Wunderlich, S. Z. D. Cheng and M. A. Yandrasits, Polymers for Advanced

- Technology, 5 (1994) 785; J. Cheng, Y. Jin, G. Liang, B. Wunderlich, and H. G. Wiedemann, *Mol. Cryst., Liq. Cryst.*, 213 (1992) 237.
- 4 B. Wunderlich, *J. Polymer Sci., Part C*, 1 (1963) 41.
- 5 J. Grebowicz, H. Suzuki and B. Wunderlich, *Polymer*, 26 (1985) 561.
- 6 U. Gaur and B. Wunderlich, *J. Phys. Chem., Ref. Data*, 10 (1981) 119.
- 7 B. Wunderlich, *J. Chem. Phys.*, 37 (1962) 1203.
- 8 Y. Kim, H. L. Strauss and R. G. Snyder, *J. Phys. Chem.*, 93 (1989) 7520.
- 9 B. G. Sumpter, D. W. Noid, G. L. Liang and B. Wunderlich, *Adv. Polymer Sci.*, 116 (1994) 27.
- 10 Yu. V. Cheban, S. F. Lau and B. Wunderlich, *Coll. Polym. Sci.*, 260 (1982) 9.
- 11 D. W. Noid, M. Varma-Nair, B. Wunderlich and J. A. Darsey, *J. Thermal Anal.*, 37 (1989) 2295.
- 12 C. E. Hecht, *Statistical Thermodynamics and Kinetic Theory*, Ch. 4, W. H. Freeman and Co., 1990; M. Blackman, *Enc. of Physics*, Ed. S. Flügge, Vol. III, Part I, Springer, Berlin 1955.
- 13 B. Wunderlich and H. Baur, *Adv. Polym. Sci.*, 7 (1970) 151.
- 14 S.-F. Lau and B. Wunderlich, *J. Thermal Anal.*, 28 (1982) 59.
- 15 R. Pan, M. Varma-Nair and B. Wunderlich, *J. Thermal Anal.*, 35 (1989) 951.
- 16 S. S. M. Wong, *Computational Methods in Physics and Engineering*. Prentice Hall, New York, NY, 1992.
- 17 T. N. L. Patterson, *The Optimum Addition of Points to Quadrature Formulae*. *Math. Comp.*, 22 (1968) 847.
- 18 The NAG Fortran Library, Mark 15, The Numerical Algorithms Group Limited, 1991.
- 19 J. M. Zurada, *Introduction to Artificial Neural Systems*, West Publishing Company, New York, NY, 1992.
- 20 H. S. Bu, S. Z. D. Cheng and B. Wunderlich, *J. Phys. Chem.*, 91 (1987) 4179.